

Helium damage in metal-tritium systems

O. Blaschko, J. Pleschiutchnig, R. Glas, and P. Weinzierl

Institut für Experimentalphysik, Universität Wien, Strudlhofgasse 4, A-1090 Wien, Austria

(Received 17 January 1991)

The time evolution of Debye-Scherrer lines was investigated in metal-tritium-helium systems by neutron-scattering techniques. Polycrystalline samples of TaT_x , YT_x , and ScT_x were measured over a period of three years. The results show that helium damage is governed by the behavior of self-interstitial atoms and dislocation loops created by helium clustering and bubble formation. The self-interstitials and loops induce a lattice expansion in the early stages of helium formation. For higher helium concentrations the self-interstitials and loops produced are completely incorporated into an evolving dislocation network. In hexagonal rare-earth systems a preferential condensation of loops into a dislocation network lying in basal planes is observed. Additional small-angle-scattering experiments show that platelike helium cavities are formed in the hexagonal systems.

I. INTRODUCTION

Helium damage in materials is an important problem for future fusion reactor technology.¹ The implantation of helium atoms with high energies or helium production due to the radioactive decay of tritium induces a defect structure generally influencing the mechanical properties of the first wall material. Metal-helium systems are solid-state systems in which the defect structure shows a continuous evolution with increasing helium concentration and connected helium clustering and bubble formation.

Most of the experiments on helium damage were done by electron microscopy methods, revealing features of bubble formation.² Only a few works deal with scattering methods, which, however, give more integral information on the lattice distortions and defect structure involved. Recently, in two separate investigations the lattice deformation of TaT_xHe_y systems was studied by the measurement of the evolution of diffraction peaks, i.e., peak shifts and broadening with increasing helium concentration.³⁻⁵ Both investigations reveal the creation of self-interstitials and dislocation loops followed by the formation of a dislocation network in TaT_xHe_y at room temperature.

In the present work we continue our neutron-scattering investigations of Debye-Scherrer lines in TaT_xHe_y .⁵ We present observations for higher helium concentrations. Second, we have extended our measurements to rare-earth-tritium systems with the aim to investigate the evolution of the defect structure within a hexagonal metal matrix. Finally, additional neutron small-angle-scattering results revealing the formation of plate-like helium cavities in the rare-earth metals are also presented.

II. EXPERIMENT

Debye-Scherrer line measurements were performed on the triple-axis spectrometer VALSE located at a cold-

neutron guide position at the Laboratoire Léon Brillouin in Saclay, France. An incident neutron wavelength of 2.36 Å was chosen, and a pyrolytic graphite filter was put into the incident beam. Collimations of 10 min before and after the sample were used. In order to reduce texture effects, the polycrystalline samples were rotated continuously during the experiment. Additional investigations were undertaken by small-angle-scattering techniques on the spectrometer PAXE, where a multidetector system is installed.

The samples were polycrystalline platelets ($1 \times 10 \times 50$ mm³) of tantalum, scandium, and yttrium, respectively. The samples were loaded with tritium from the gas phase. At the obtained initial tritium concentrations, all metal-tritium systems remained in the solid-solution phase at room temperature. The tantalum platelet had an initial tritium concentration of 4 at. %. A Sc and a Y platelet were loaded with 14.2 and 8.9 at. % tritium, respectively. After the loading procedure these samples were mounted into a high-vacuum sealed cylindrical aluminum container with a wall thickness of 1 mm and kept at room temperature. The container for the Sc and Y samples was provided with quartz windows, also allowing a small-angle-scattering investigation. Moreover, a second yttrium platelet was loaded with 6.8 at. % tritium and then mounted into a liquid-nitrogen cryostat and kept there during the whole period of investigation. Because of the peculiar yttrium-hydrogen phase diagram, this YT_x sample also remained in the solid-solution phase even at liquid-nitrogen temperature.⁶

III. DEBYE-SCHERRER LINES

The Debye-Scherrer lines were measured in function of time and helium concentration in all metal-tritium systems. The measurements were performed over a period of several years. In order to get a constant reference over the whole time period, similar platelets of the corresponding pure metals were measured each time for comparison. The position and width of the Debye-Scherrer lines were determined by Gaussian fits to the data. In all

cases, even in samples with higher helium concentrations, the measured profile of the Debye-Scherrer lines could well be described by a Gaussian. The broadening of the line was then obtained by a Gaussian deconvolution with the linewidth measured in the pure metal. In the following the results for the helium-induced lattice expansion and line broadening are presented for the four systems investigated. The values for the lattice expansion observed are corrected for the known lattice contraction due to tritium decay.

A. TaT_x system

The helium-induced lattice expansion corrected for the contraction due to tritium decay is shown in Fig. 1. First, for lower concentrations a lattice-parameter increase is found. The lattice expansion then saturates and is followed for higher helium concentrations by a slight lattice parameter decrease. For comparison the figure shows also recent results of the Jülich group on a higher-concentrated TaT_x system (i.e., $x = 0.165$).⁴ Qualitatively, a similar lattice parameter behavior is observed. The figure shows, however, that in our lower-concentrated TaT_x system the initial lattice expansion is steeper, but ceases at a much lower helium concentration.

The line-broadening results are shown in Fig. 2. From

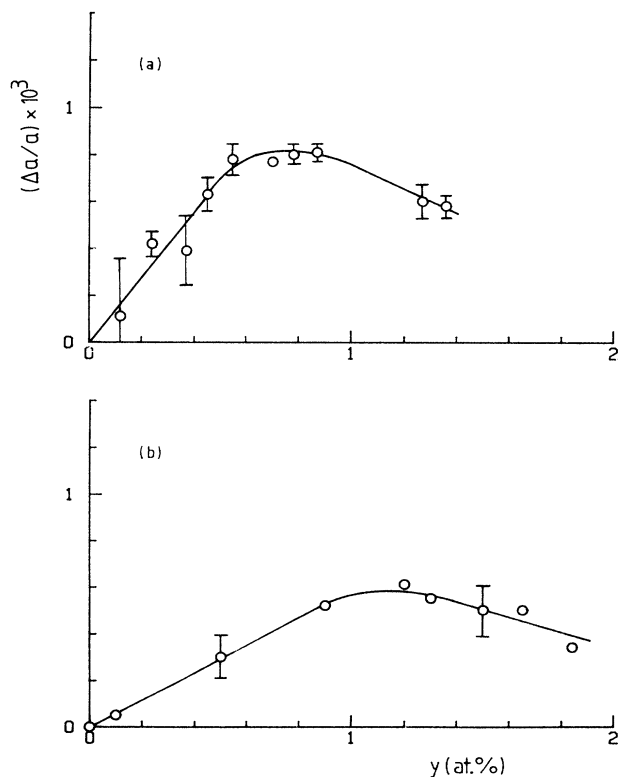


FIG. 1. (a) The helium-induced relative lattice-parameter change as a function of helium concentration y (at. %) for a TaT_{0.04} system. (b) For comparison the results of Ref. 4 for TaT_{0.165} are shown. The data are corrected for the known lattice contraction due to tritium decay.

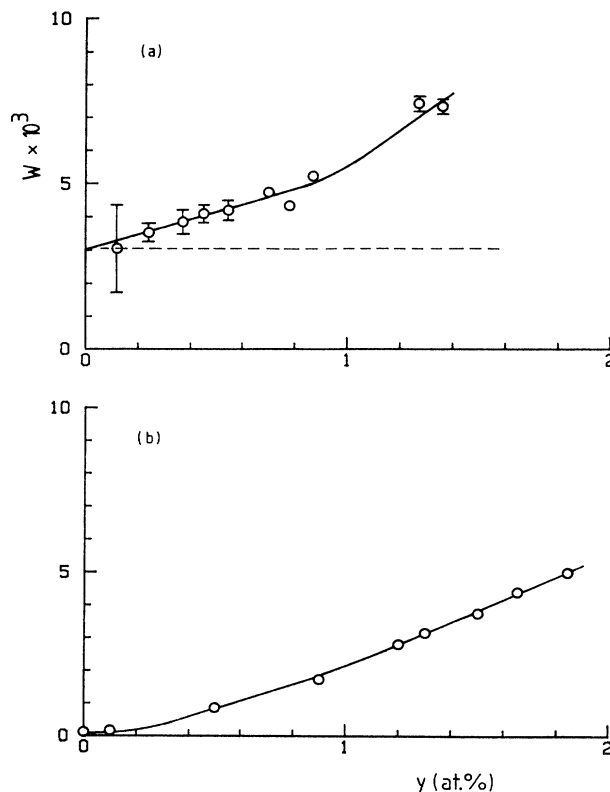


FIG. 2. Relative broadening of Debye-Scherrer lines (W) vs. helium concentration y (at. %) in TaT_{0.04}. The data points indicate average values obtained from three reflections, i.e., (002), (110), and (211). The dashed line indicates the zero level if the first measured point is taken as reference. (b) For comparison the results of Ref. 4 are shown for the (222) reflection in TaT_{0.165}.

low helium concentrations a continuous increase of the linewidths is observed. The data show a finite value for the line broadening in the limit of helium concentrations toward zero. This feature was also found in all other systems after tritium loading and may therefore be ascribed to dislocation generation by the loading process. If the line broadening obtained for $y=0$ is taken as the zero level, then the present results are in rather good agreement with corresponding data from the Jülich group obtained on a single crystal with a different scattering method.⁴

We should further note that during this experiment the TaT_x platelet began to break into pieces at about 0.5 at. % helium. This macroscopic disintegration continued with further helium increase.

B. ScT_x system

The helium-induced dilatation of the hexagonal ScT_x lattice is shown in Fig. 3. First, a volume increase is observed; then, near 0.8 at. % helium, the lattice expansion levels off and remains constant for higher concentrations.

The line-broadening measurements in ScT_x gave results shown in Fig. 4. A continuous linewidth increase is

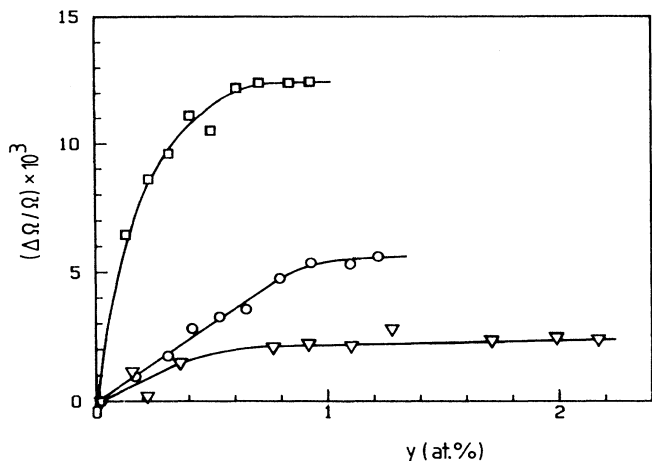


FIG. 3. Relative dilatation of the hexagonal systems vs helium concentrations y (at. %) [$\text{ScT}_{0.142}$ (∇), $\text{YT}_{0.089}$ aged at room temperature (\circ), and $\text{YT}_{0.068}$ aged at liquid-nitrogen temperature (\square). The data are corrected for the known lattice contraction due to tritium decay.

observed for reflections lying in the basal plane. The linewidths of the reflections along the hexagonal direction show, however, a drastic steplike increase near 0.8 at. % helium. After the step region the widths of the hexagonal reflections show a steeper increase than the reflections in the basal plane. In ScT_x reflections along intermediate directions between the hexagonal direction and basal plane were also investigated. Their linewidths show a similar but smaller discontinuity as observed for the $(00.l)$ direction. It is interesting to note that the step in the linewidths of the $(00.l)$ reflections occurs in the same concentration range where the lattice expansion saturates.

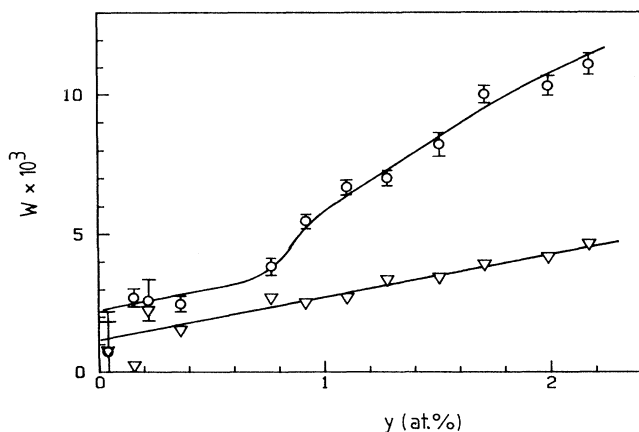


FIG. 4. Relative broadening of Debye-Scherrer lines in $\text{ScT}_{0.142}$ vs helium concentration y (at. %). The hexagonal (00.2) reflection (\circ) and reflections in the basal plane (∇).

C. YT_x systems

The YT_x sample kept at room temperature (Fig. 3) shows qualitatively a similar behavior as observed for the ScT_x system. First, a helium-induced lattice dilatation is observed. The dilatation then saturates near 0.8 at. % and remains constant for higher helium concentrations. The amount of the lattice dilatation in YT_x at room temperature (Fig. 5) is, however, much higher than previously described for the ScT_x system.

The line-broadening measurements for the YT_x sample aged at room temperature (Fig. 5) revealed a similar concentration dependence as observed in ScT_x . Especially, a steplike increase in the linewidths is found for reflections parallel to the hexagonal direction. As in ScT_x , the step occurs in YT_x in the same concentration range where the lattice expansion saturates.

The YT_x sample held at liquid-nitrogen temperature (Fig. 3) also exhibits in the lower-concentration range a helium-induced lattice dilatation, which is, however, the strongest one observed in this experiment. This lattice dilatation also ceases at higher concentrations. In the sample kept at liquid-nitrogen temperature, the line-broadening measurements (Fig. 6) showed, besides the initial broadening observed for all tritium-loaded samples near $y=0$, however, no further evolution of the Debye-Scherrer linewidth.

To conclude this section we should note that, during these investigations of hexagonal rare-earth-tritium systems reaching helium concentrations up to 2.6 at. %, no macroscopic fracture of the platelets was observed.

IV. SMALL-ANGLE-SCATTERING RESULTS

The helium-cavity morphology in the rare-earth tritides aged at room temperature was investigated by some additional neutron small-angle-scattering experiments.

Below 0.8 at. % helium, no conclusive results could be

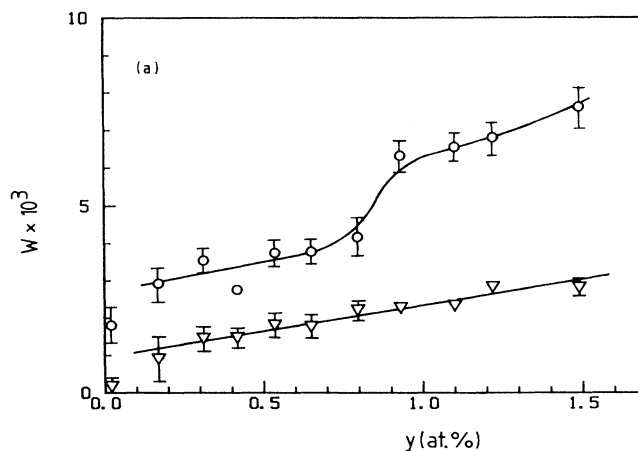


FIG. 5. Relative broadening of Debye-Scherrer lines (W) in $\text{YT}_{0.089}$ at room temperature vs helium concentration y (at. %). The hexagonal (00.2) reflection (\circ) and reflections in the basal plane (∇).

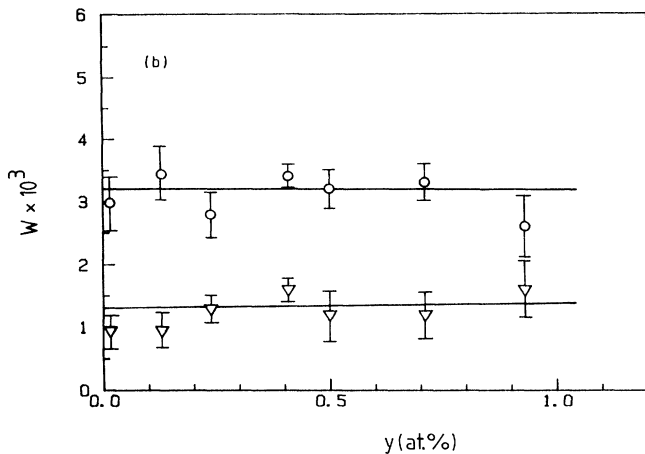


FIG. 6. Relative line broadening (W) in $YT_{0.068}$ kept at liquid-nitrogen temperature. (00.2) reflection (\circ) and reflections in the basal plane (∇). As in all other systems, the tritium-loading procedure apparently induced an initial line broadening, which, however, shows no further evolution.

obtained. Above 0.8 at. % helium, however—i.e., above the steplike increase in the linewidths along the c direction—small-angle-scattering intensity was observed in both systems.

In ScT_x at a helium concentration of 1.28 at. %, isotropic small-angle scattering was observed in the (x, y)

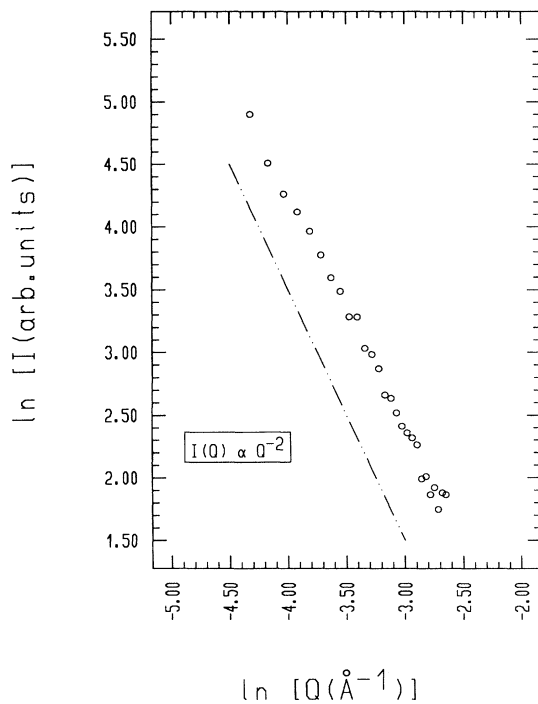


FIG. 7. Small-angle-scattering intensity distribution in ScT_x with a helium concentration of 1.28 at. % shown in a double-logarithmic [$\ln(I)$ vs $\ln(Q)$] plot. The dot-dashed line shows a Q^{-2} dependence.

multidetector system. The scattered intensity showed a linear dependence in a double-logarithmic plot ($\ln I$, $\ln Q$) with a slope of -2 (Fig. 7). This $I \sim Q^{-2}$ behavior is the signature of platelike cavities in a small-angle-scattering pattern.⁷

On the other hand, an investigation of the YT_x system at a helium concentration of 1.10 at. % revealed a strongly anisotropic scattering in reciprocal space. Figure 8 shows intensity streaks by iso-intensity contours. In an additional experiment it was established that the symmetry of the streaks corresponds to the symmetry of the texture of the polycrystalline Y materials; i.e., the intensity streaks point into the hexagonal c direction of the Y lattice. Similar starlike intensity patterns were also observed in YT_x at higher helium concentrations. In small-angle-scattering experiments on single crystals or polycrystals with preferred orientations, intensity streaks are produced by inclusions with a platelike morphology. The intensity pattern of Fig. 7 therefore gives evidence that platelike helium cavities lying in the basal plane are formed in YT_x at higher helium concentrations.

V. DISCUSSION

The following general features of the lattice deformation in metal-tritium-helium systems are revealed by the present series of experiments.

Besides quantitative differences, all systems expand their lattice in the early stages of helium formation. This evolution ceases at higher concentrations.

Second, a broadening of Debye-Scherrer lines is generally observed with the only exception being the YT_x sample aged at liquid-nitrogen temperature. This broadening increases with increasing helium concentration. In the hexagonal rare-earth systems, the line

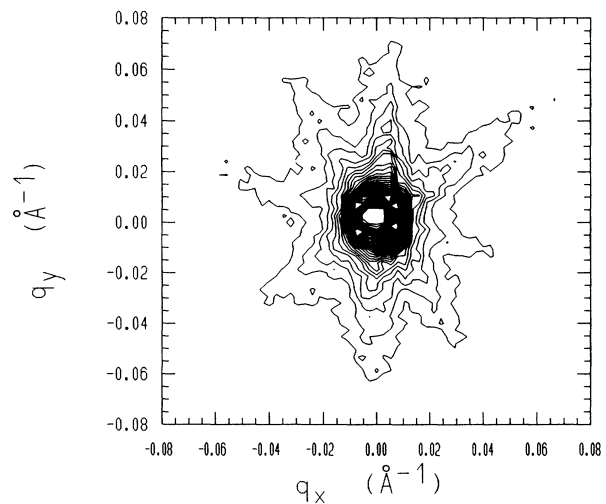


FIG. 8. Small-angle-scattering intensity distribution observed in YT_x with a helium concentration of 1.1 at. % aged at room temperature. The distribution is shown by equally spaced iso-intensity contours. The streaks point into hexagonal (00.2) directions.

broadening is strongly anisotropic and shows especially a steplike increase near 0.8 at. % He for reflections along the hexagonal direction.

Furthermore, the small-angle-scattering data show that platelike helium cavities are formed at room temperature in the hexagonal rare-earth systems.

The helium evolution in metal-tritium systems is generally seen as follows. The helium atoms produced continuously by tritium decay form clusters and then helium bubbles. The bubble formation is inherently connected with the production of self-interstitials at low temperatures with respect to the melting point where thermal vacancies are not available.^{13,14} These metal atoms remain bound to the bubble until they are punched out as dislocation loops. The continuous formation of dislocation loops finally leads to the creation of a dislocation network.

From general considerations of scattering theory,⁸ it follows that defects of infinite size such as dislocations and dislocation networks induce a broadening of Bragg reflections or Debye-Scherrer lines. On the other hand, lattice defects of finite size, i.e., interstitials and isolated dislocation loops, have no effect on the linewidth, but induce peak shifts and diffuse scattering.

In terms of this classification the present results show that dislocations are formed in all samples at room temperature because of low helium concentrations. The dislocation density increases with increasing helium concentration as borne out by the Debye-Scherrer linewidth behavior.

The lattice expansion observed in all systems at lower helium concentrations can be related to the emission of self-interstitials and dislocation loops during helium clustering and subsequent bubble formation. One part of the interstitials contributes to the formation of the dislocation network, inducing the line broadening observed, while another part of the interstitials remains in the matrix. At higher helium concentrations the helium-induced lattice expansion ceases, indicating that most of the interstitials produced are now incorporated into the evolving dislocation network. It is interesting to note that the turning point of the lattice expansion for all metal-tritium systems occurs roughly within a similar helium-concentration range.

Furthermore, the present experiment shows that the linewidth behavior is anisotropic in the hexagonal metals. The steplike increase of the widths observed for reflections along the hexagonal direction shows the formation of a dislocation network consisting preferentially of dislocations lying in the basal plane. The step in the linewidths occurs in the same helium-concentration range where the lattice expansion saturates and therefore confirms the result that the saturation of the lattice dilatation indicates the complete integration of interstitials and loops into a network structure.

Moreover, the lattice expansion saturates at a much lower value in ScT_x than in YT_x, indicating that the tendency of dislocation loops to form straight dislocations on basal plane is more pronounced in the first. This increased tendency in ScT_x may be favored from elastic-energy considerations as oppositely to yttrium the hexag-

onal direction is the stiff one in Sc.

The anisotropic properties of the hexagonal rare-earth lattices likewise determine the helium-cavity morphology. In YT_x and ScT_x platelike helium cavities were observed by small-angle scattering. In YT_x the anisotropic scattering pattern showed that the platelike cavities are also lying in the basal plane of the hexagonal lattice. According to Ref. 9, platelike precipitates are formed in order to reduce the coherency stresses with the metal matrix. In this case the platelets are oriented perpendicularly to the soft elastic direction. It is interesting to note that in ScT_x the platelike helium cavities, however, are lying perpendicularly to the stiff hexagonal direction.

A comparison of the present TaT_x results with that of the Jülich group⁴ show, despite a qualitatively similar behavior, some quantitative differences. In our TaT_x system with the lower tritium concentration the initial lattice expansion is steeper, but ceases at a lower helium concentration. This difference shows, of course, that the created defect structure may depend also on the tritium concentration. The higher helium-generation rate in the higher-concentrated TaT_x system may lead to an increased self-trapping of helium atoms and consequently to a higher density of helium bubbles. It seems therefore that a finer distribution of smaller helium bubbles favors an easier integration of the emitted self-interstitials and loops into the dislocation network structure. Furthermore, both TaT_x investigations show after the turning point of the lattice expansion a decrease of the lattice dilatation at higher helium concentrations. This behavior is not observed in the rare-earth tritides, where the lattice dilatation remains essentially constant at higher helium concentrations. In Ref. 4 it was argued that this lattice-parameter decrease is induced by an increased tritium trapping on the created defect structure. Alternatively, it may be possible that a part of the isolated defects which are responsible for the lattice expansion observed are also incorporated into the network structure at higher concentrations.

Finally, the results obtained on the YT_x sample aged at liquid-nitrogen temperature support, especially for the early stages of helium formation, the general defect-structure behavior described. At liquid-nitrogen temperature the helium atoms are still mobile and helium clustering with its concomitant emission of self-interstitials and loops seems to occur. The mobility of the interstitials is, however, strongly reduced,¹⁵ and no dislocation network is created as shown by the absence of an evolution of the measured linewidths. As no interstitials are transferred to a dislocation network, the lattice expansion is the strongest one in YT_x at liquid-nitrogen temperature. The lattice expansion observed in the initial stages of helium formation is roughly in agreement with the high values for the relative lattice dilatation induced by self-interstitials in hexagonal systems.¹⁰

On the other hand, in the cold YT_x sample the lattice expansion also ceases at higher helium concentrations without, however, a connected broadening of the Debye-Scherrer lines. This remarkable result is an exception in view of the general behavior found at room temperature.

If it is assumed that helium clustering still occurs, then one must conclude that the self-interstitial emission is strongly reduced in this helium-concentration range, indicating a preferential clustering near defects, e.g., small bubbles on dislocation loops.¹¹ Tentatively, it may also be conjectured that further helium-bubble growth and subsequent self-interstitial emission is inhibited by the high density of dislocation loops already produced and retained in the matrix at liquid-nitrogen temperatures. This last behavior is discussed in a recent theoretical investigation.¹²

In summary, the present investigation shows that at lower temperatures the defect structure induced by helium clustering can be described in terms of a balance between self-interstitials (or loops) and a interconnected

dislocation network. The defect structure depends on temperature and is strongly influenced by the symmetry and elastic anisotropy of the metal matrix.

ACKNOWLEDGMENTS

The authors would like to thank H. Trinkaus from Jülich for valuable discussions. Our work was partly supported by the Bundesministerium für Wissenschaft und Forschung and the Fonds zur Förderung der wissenschaftlichen Forschung, Austria. The Laboratoire Léon Brillouin is a joint research institute of the Centre National de la Recherche Scientifique and the Commissariat à l'Énergie Atomique, France.

¹H. Ullmaier, Nucl. Fusion **24**, 1039 (1984).

²See, e.g., J. H. Evans, A. Van Veen, and L. M. Caspers, Radiat. Eff. **78**, 105 (1983).

³R. Laesser, K. Bickmann, and H. Trinkaus, Phys. Rev. B **40**, 3306 (1989).

⁴R. Laesser, K. Bickmann, H. Trinkaus, and H. Wenzl, Phys. Rev. B **34**, 4364 (1986).

⁵O. Blaschko, G. Ernst, P. Fratzl, G. Krexner, and P. Weinzierl, Phys. Rev. B **34**, 4985 (1986).

⁶J. P. Burger, J. N. Daou, A. Lucasson, and P. Vajda, Z. Phys. Chem. **143**, 111 (1985).

⁷See, e.g., A. Guinier and G. Fournet, *Small Angle Scattering of X-Rays* (Wiley, New York 1955).

⁸M. A. Krivoglaz, *Theory of X-ray and Thermal Neutron Scattering by Real Crystals* (Plenum, New York, 1969).

⁹A. G. Khachaturyan, *Theory of Structural Transformations in Solids* (Wiley, New York, 1983).

¹⁰P. Ehrhart and B. Schoenfeld, Phys. Rev. B **19**, 3896 (1979).

¹¹W. Kesternich, Radiat. Eff. **78**, 261 (1983).

¹²W. G. Wolfer, Philos. Mag. A **59**, 87 (1989).

¹³W. D. Wilson, C. L. Bisson, and M. I. Baskes, Phys. Rev. B **24**, 5616 (1981).

¹⁴H. Trinkaus and W. G. Wolfer, J. Nucl. Mater. **122&123**, 552 (1984).

¹⁵J. N. Daou, P. Vajda, A. Lucasson, and P. Lucasson, J. Phys. F **10**, 583 (1980).